Supplementary Material

Stability/Activity Tradeoffs in *Thermus thermophilus* Laccase

Jieun Shin, Harry B. Gray* and Jay R. Winkler*
Beckman Institute,
California Institute of Technology, Pasadena CA USA 91125

Protein Preparation

Tth-lac was expressed in *E. coli* and purified following the published method [1] with slight modifications. To sum up, the plasmid was prepared by cloning the *Tth*-lac encoding region into the pET22b expression vector at NdeI digestion site. *Tth*-lac with a N-terminal 6 x His-tag was transformed into BL21(DE3) cells on a LB/Amp agar plate. Single colonies grown on the plate were inoculated in 5mL TB/Amp at 37˚C for 5-7 hours (starter culture), and the frozen stock was prepared for later use. The cells were pelleted and re-inoculated in 4-6L of TB/Amp/0.4% glycerol at 37˚C overnight. Protein expression was achieved after induction with IPTG at 37˚C for 7-8 hours. After the induction, cells were harvested by centrifugation and were kept at -20˚C until use.

The frozen cell pellets were thawed and the cells were resuspended in 20mM Tris buffer at pH 8 with the addition of protease inhibitors (Complete Mini Protease Inhibitor Cocktail Tablets, Pefabloc SC (AEBSF) and Benzamidine hydrochloride hydrate). The enzyme was released by sonicating the cells for an hour, and the sample was centrifuged to remove all the cell debris. The supernatant solution after centrifugation was further purified by heating to approximately 65˚C for 20 min. At this temperature, the majority of other *E. coli* enzymes precipitate due to thermal denaturation, and *Tth*-lac remains in solution. All precipitates were removed by centrifugation. Since the recombinant *Tth*-laccase has an N-terminal 6 x His-tag, a nickel immobilized metal affinity column (IMAC) was used to bind the protein. Remnants of undesired *E. coli* proteins eluted first from the IMAC column with wash and load buffers. The *Tth*-laccase eluted with increasing concentration of imidazole in the elution buffer. After protein metalation, a cation exchange column (HiPrep SP HP 16/10 column) was used to remove additional impurities by selectively collecting the fraction of interest monitored by absorption at 280 and 605 nm.

Circular Dichroism Spectra

Circular dichroism spectra of the protein samples under N_2 were recorded on an Aviv model 430 circular dichroism spectrometer from 260 to 190 nm to monitor conformational changes and/or thermal denaturation over the temperature range 20 to 65˚C. Measurements were made on 3 µM protein in 20 mM sodium phosphate buffer, pH 6.

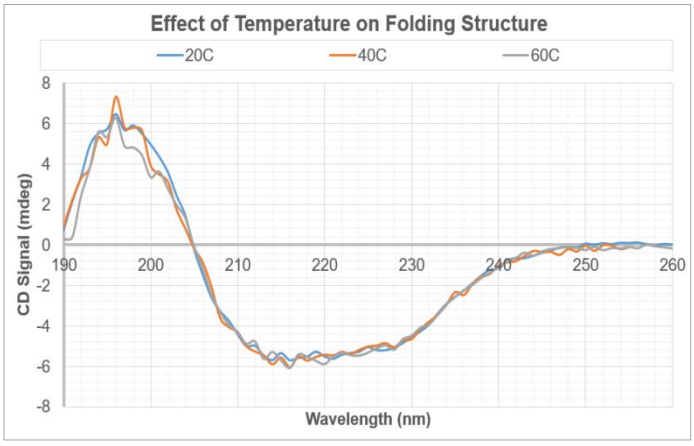

Figure S1. Circular dichroism spectra of *Tth*-lac from 20 to 65˚C

Synthesis of $[Ru(NH_3)_4(bpy)](PF_6)_2$

$[Ru(NH_3)_4(bpy)](PF_6)_2$ was synthesized and characterized following a published protocol (with slight modifications) [2]. Zinc amalgam was prepared with mercuric chloride ($HgCl_2$) and mossy zinc; $[Ru(NH_3)_5Cl]Cl_2$ was purchased from STREM chemicals INC. All the procedures were performed under argon using Schlenk-line techniques.

Estimation of the Cu_{T1} Potential from Redox Equilibria

A 60 μM wild-type *Tth*-laccase sample and four reducing equivalents of (240 uM) $[Ru(NH_3)_4(bpy)](PF_6)_2$ were separately deoxygenated by gentle vacuum/argon pump and backfill cycles and were then mixed together in a sealed quartz cuvette. The UV-Vis spectra of the mixed sample were monitored from 20 to 65˚C in the absorption regions at 366, 525 and 605 nm (the λ_{max} values of $Ru(NH_3)_4(bpy)](PF_6)_2$ and the T1 copper, respectively). Equilibrium concentrations of Cu_{T1}^{2+} and Ru^{2+} in the mixed sample were determined by least squares decomposition of the mixed spectrum into a linear combination of the two component spectra. The spectra of $[Ru(NH_3)_4(bpy)](PF_6)_2$ and the wild type protein were monitored separately at different temperatures to account for temperature dependent changes in the component spectra.

$[Ru(NH_3)_4(bpy)](PF_6)_2$	Cu_{T1} in Wild Type Protein
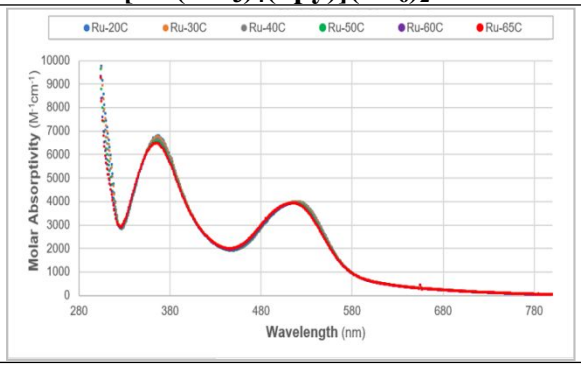	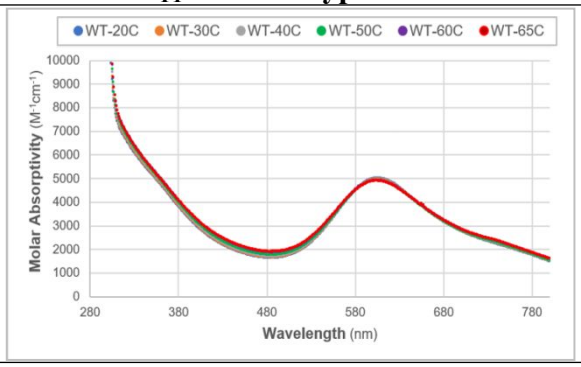
• λ_{max} = 366nm (ε = 6380$M^{-1}cm^{-1}$) [2] • λ_{max} = 525nm (ε = 3950$M^{-1}cm^{-1}$) [2]	• λ_{max} = 605nm (ε = 5020$^{-1}cm^{-1}$)

Figure S2. UV-vis spectra (20 to 65˚C) for deoxygenated samples of $[Ru(NH_3)_4(bpy)](PF_6)_2$ and of wild type *Tth*-lac.

Table S1. Temperature dependent equilibrium concentrations of Cu^{1+}, Cu^{2+}, Ru^{2+} and Ru^{3+}

	293K	303K	313K	323K	333K	338K
$[Cu^{2+}]$ (uM)	44.6	48.3	52.1	55.1	56.7	57.1
$[Cu^{1+}]$ (uM)	15.4	11.7	7.9	4.9	3.3	2.9
$[Ru^{2+}]$ (uM)	123.1	126.5	132.6	142.7	152.0	160.1
$[Ru^{3+}]$ (uM)	117.0	113.5	107.4	97.3	88.0	79.9

$A_{525} = \varepsilon_{Ru525}[Ru^{2+}] + \varepsilon_{Cu525}[Cu^{2+}]$
$A_{605} = \varepsilon_{Ru605}[Ru^{2+}] + \varepsilon_{Cu605}[Cu^{2+}]$

$Cu^{2+} + Ru^{2+} \rightleftharpoons Cu^{+} + Ru^{3+}$

$$K_{eq} = \frac{[Cu^{+}][Ru^{3+}]}{[Cu^{2+}][Ru^{2+}]}$$

$$K_{eq} = exp\left\{\frac{-\Delta G^{\circ}}{RT}\right\}$$

$$\Delta G^{\circ} = -RTlnK$$

$$\Delta E^{\circ} = -\frac{\Delta G^{\circ}}{F} = E^{\circ}(Cu^{2+/+}) - E^{\circ}(Ru^{3+/2+})$$

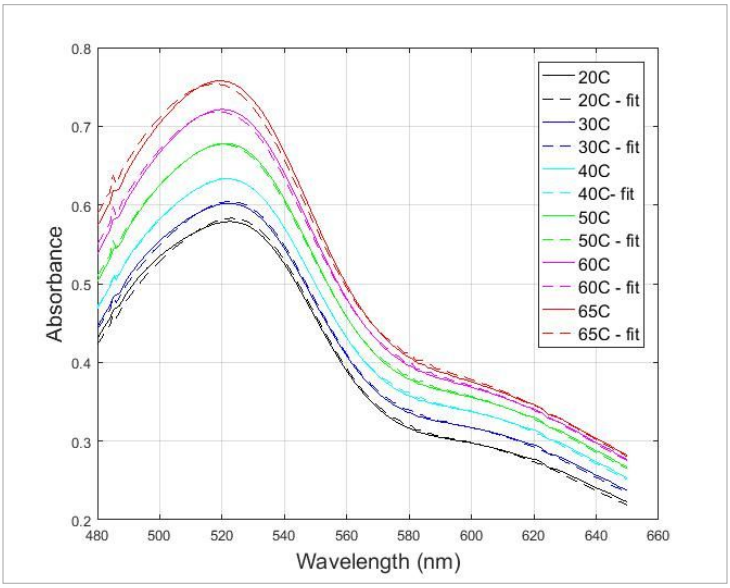

Figure S3. Equilibrium concentrations of $[Ru^{2+}]$, $[Ru^{3+}]$, $[Cu^{2+}]$ and $[Cu^{+}]$ were obtained from global fitting of the redox titration data. Spectra of the wild type protein and $[Ru(NH_3)_4(bpy)](PF_6)_2$ obtained every 10 ˚C from 20 to 60 ˚C (also at 65 ˚C) monitor concentration changes at the different temperatures.

Error Propagation

$$\mathbf{K_{eq} = ([Cu^{2+}]_0 - [Cu^{2+}])*([Ru^{2+}]_0 - [Ru^{2+}])/([Cu^{2+}]*[Ru^{2+}])}$$

- All concentrations are in μM.
- $[Cu^{2+}]_0$ = initial concentration of *Tth*-lac
- $[Cu^{2+}]$ = final concentration of *Tth*-lac
- $[Ru^{2+}]_0$ = initial concentration of $[Ru(NH_3)_4(bpy)](PF_6)_2]$
- $[Ru^{2+}]$ = final concentration of $[Ru(NH_3)_4(bpy)](PF_6)_2]$
- lb uncertainty: lower bound uncertainty (95% confidence interval)
- ub uncertainty: upper bound uncertainty (95% confidence interval)

Temperature (K)	293	303	313	323	333	338
$[Cu^{2+}]_0$	6.00E-05	6.00E-05	6.00E-05	6.00E-05	6.00E-05	6.00E-05
$[Cu^{2+}]_0$ lb uncertainty	1.00E-07	1.00E-07	1.00E-07	1.00E-07	1.00E-07	1.00E-07
$[Cu^{2+}]_0$ ub uncertainty	1.00E-07	1.00E-07	1.00E-07	1.00E-07	1.00E-07	1.00E-07
$[Cu^{2+}]$	4.46E-05	4.83E-05	5.21E-05	5.51E-05	5.67E-05	5.71E-05
$[Cu^{2+}]$ lb uncertainty	2.03E-07	1.64E-07	7.00E-08	8.40E-08	1.96E-07	3.11E-07
$[Cu^{2+}]$ ub uncertainty	1.97E-07	1.36E-07	1.30E-07	1.16E-07	2.04E-07	2.89E-07
$[Ru^{2+}]_0$	2.40E-04	2.40E-04	2.40E-04	2.40E-04	2.40E-04	2.40E-04
$[Ru^{2+}]_0$ lb uncertainty	5.00E-07	5.00E-07	5.00E-07	5.00E-07	5.00E-07	5.00E-07
$[Ru^{2+}]_0$ ub uncertainty	5.00E-07	5.00E-07	5.00E-07	5.00E-07	5.00E-07	5.00E-07
$[Ru^{2+}]$	1.23E-04	1.27E-04	1.33E-04	1.43E-04	1.52E-04	1.60E-04
$[Ru^{2+}]$ lb uncertainty	3.50E-07	2.10E-07	1.10E-07	2.10E-07	3.60E-07	5.40E-07
$[Ru^{2+}]$ ub uncertainty	3.50E-07	2.90E-07	1.90E-07	1.90E-07	3.40E-07	4.60E-07
$([Cu^{2+}]_0 - [Cu^{2+}])$	1.54E-05	1.17E-05	7.93E-06	4.92E-06	3.30E-06	2.89E-06
$([Cu^{2+}]_0 - [Cu^{2+}])$ lb uncertainty	3.03E-07	2.64E-07	1.70E-07	1.84E-07	2.96E-07	4.11E-07
$([Cu^{2+}]_0 - [Cu^{2+}])$ ub uncertainty	2.97E-07	2.36E-07	2.30E-07	2.16E-07	3.04E-07	3.89E-07
$([Ru^{2+}]_0 - [Ru^{2+}])$	1.17E-04	1.13E-04	1.07E-04	9.73E-05	8.80E-05	7.99E-05
$([Ru^{2+}]_0 - [Ru^{2+}])$ lb uncertainty	8.50E-07	7.10E-07	6.10E-07	7.10E-07	8.60E-07	1.04E-06
$([Ru^{2+}]_0 - [Ru^{2+}])$ ub uncertainty	8.50E-07	7.90E-07	6.90E-07	6.90E-07	8.40E-07	9.60E-07
$([Cu^{2+}]_0 - [Cu^{2+}])*([Ru^{2+}]_0 - [Ru^{2+}])$	1.80E-09	1.33E-09	8.52E-10	4.78E-10	2.91E-10	2.31E-10
$([Cu^{2+}]_0 - [Cu^{2+}])*([Ru^{2+}]_0 - [Ru^{2+}])$ lb uncertainty	4.85E-11	3.83E-11	2.31E-11	2.14E-11	2.89E-11	3.58E-11
$([Cu^{2+}]_0 - [Cu^{2+}])*([Ru^{2+}]_0 - [Ru^{2+}])$ ub uncertainty	4.78E-11	3.61E-11	3.02E-11	2.44E-11	2.95E-11	3.38E-11

Temperature (K)	293	303	313	323	333	338
$([Cu^{2+}]*[Ru^{2+}])$	5.49E-09	6.11E-09	6.91E-09	7.86E-09	8.62E-09	9.15E-09
$([Cu^{2+}]*[Ru^{2+}])$ lb uncertainty	4.06E-11	3.09E-11	1.50E-11	2.36E-11	5.02E-11	8.06E-11
$([Cu^{2+}]*[Ru^{2+}])$ ub uncertainty	3.99E-11	3.12E-11	2.71E-11	2.70E-11	5.03E-11	7.26E-11
K_{eq}	3.28E-01	2.18E-01	1.23E-01	6.08E-02	3.38E-02	2.52E-02
K_{eq} lb uncertainty	1.13E-02	7.37E-03	3.61E-03	2.90E-03	3.55E-03	4.14E-03
K_{eq} ub uncertainty	1.11E-02	7.02E-03	4.85E-03	3.31E-03	3.63E-03	3.90E-03
$\ln(K_{eq})$	-1.11E+00	-1.52E+00	-2.09E+00	-2.80E+00	-3.39E+00	-3.68E+00
$\ln(K_{eq})$ lb uncertainty	-3.83E-02	-5.15E-02	-6.13E-02	-1.34E-01	-3.56E-01	-6.04E-01
$\ln(K_{eq})$ ub uncertainty	-3.77E-02	-4.90E-02	-8.24E-02	-1.52E-01	-3.64E-01	-5.69E-01
$\Delta G°$ ($kJmol^{-1}$)	2.71E+00	3.84E+00	5.45E+00	7.52E+00	9.38E+00	1.03E+01
$\Delta G°$ lb uncertainty	9.42E-02	1.31E-01	1.61E-01	3.61E-01	9.90E-01	1.70E+00
$\Delta G°$ ub uncertainty	9.27E-02	1.25E-01	2.16E-01	4.12E-01	1.01E+00	1.60E+00
$\Delta E°$ (V)	-2.81E-02	-3.97E-02	-5.64E-02	-7.79E-02	-9.72E-02	-1.07E-01
$\Delta E°$ lb uncertainty	-9.76E-04	-1.36E-03	-1.67E-03	-3.74E-03	-1.03E-02	-1.76E-02
$\Delta E°$ ub uncertainty	-9.61E-04	-1.29E-03	-2.24E-03	-4.27E-03	-1.05E-02	-1.66E-02

Thermodynamic Parameters

The reaction entropy can be described by the temperature dependence of the Gibbs function.

$$\left(\frac{\delta \Delta G^{\circ}}{\delta T}\right)_{p} = -\Delta S^{\circ}$$

The reduction entropy can be described as a function of the temperature variation of E°.

$$nF\left(\frac{\delta E^{\circ}}{\delta T}\right) = \Delta S^{\circ}_{rc}$$

ΔS°: determined from the slope of the plot of ΔE° versus temperature
ΔH°: determined from the slope of the plot of ΔE°/T versus the inverse of temperature (1/T)
$\Delta S^{\circ}_{rc}(Cu^{2+/+}) = \Delta S^{\circ} + \Delta S^{\circ}_{rc}(Ru^{3+/2+})$

Table S2. Hydrophobicity of Residues within 8 Å from Cu_{T1}
(Hydrophobicity index for each amino acid residue was adopted from reference [3].)

	Hydrophobicity of Residues within 8Å from Cu	**Hydrophobicity Normalized by Total Number of Residues**	**ΔS°_{rc}** (J $mol^{-1}K^{-1}$)	**E°** (mV vs. NHE)
CPB	35.0	1.52	31	306
SBP	26.9	1.49	7	345
UmCy	33.0	1.50	-17	290
StCy	21.1	1.11	-21	265
Trv-lac	36.2	1.72	-29	738
PlCy	34.4	1.38	-36	366
AfAz	33.9	1.47	-58	266
PaAz	35.9	1.44	-68	307
Tth-lac	37.3	1.43	-120	480

Table S3. Polarity of Residues within 8Å from Cu_{T1}
(Polarity index for each amino acid residue was adopted from reference [4].)

	Polarity of Residues within 8Å from Cu	**Polarity Normalized by Total Number of Residues**	**ΔS°_{rc}** (J $mol^{-1}K^{-1}$)	**E°** (mV vs. NHE)
CPB	182	7.90	31	306
SBP	124	6.89	7	345
UmCy	369	16.8	-17	290
StCy	176	9.28	-21	265
Trv-lac	316	15.0	-29	738
PlCy	126	5.04	-36	366
AfAz	178	7.73	-58	266
PaAz	229	9.16	-68	307
Tth-lac	477	18.3	-120	480

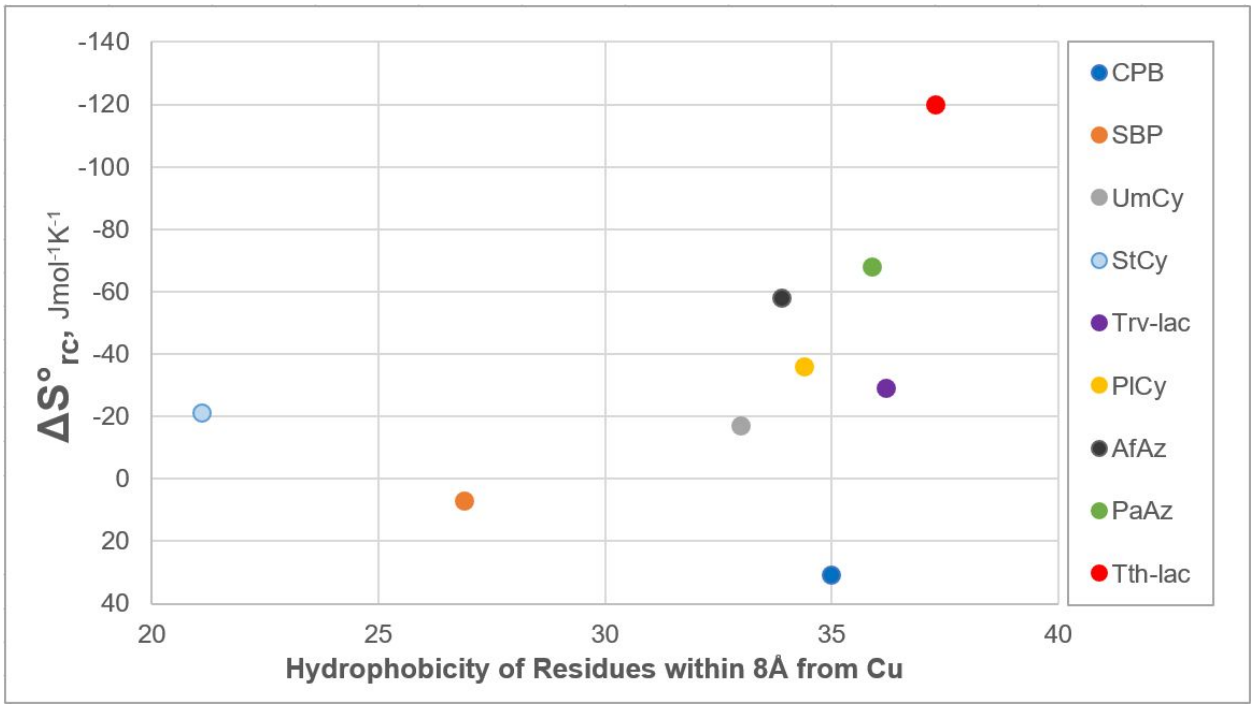

Figure S4. ΔS°_{rc} vs. Hydrophobicity of Residues within 8Å from Cu_{T1}

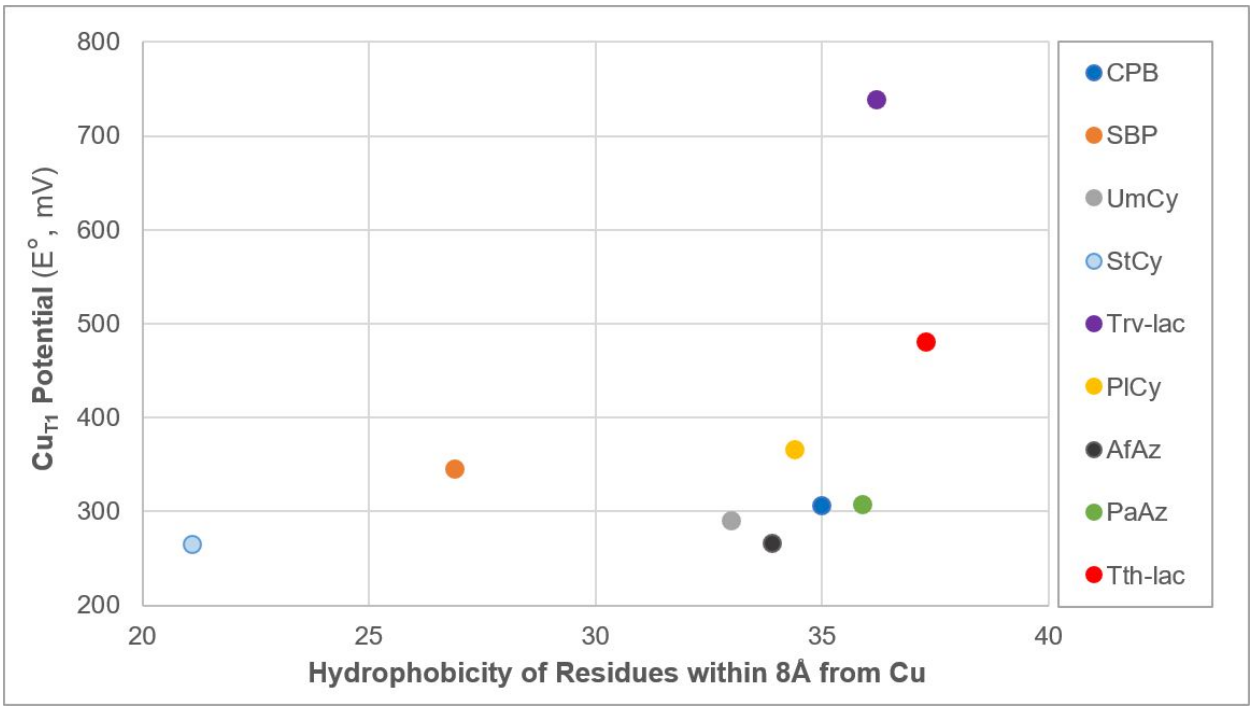

Figure S5. E° of Cu_{T1} vs. Hydrophobicity of Residues within 8Å from Cu_{T1}

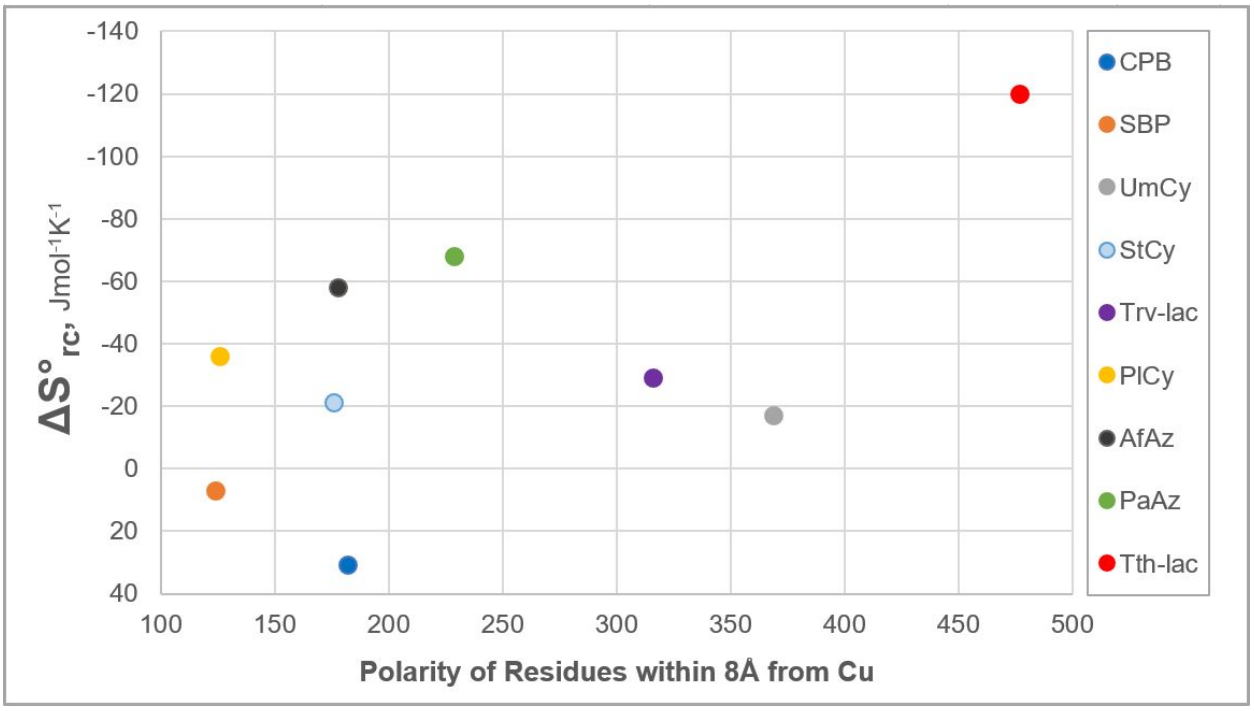

Figure S6. $\Delta S°_{rc}$ vs Polarity of Residues within 8Å from Cu_{T1}

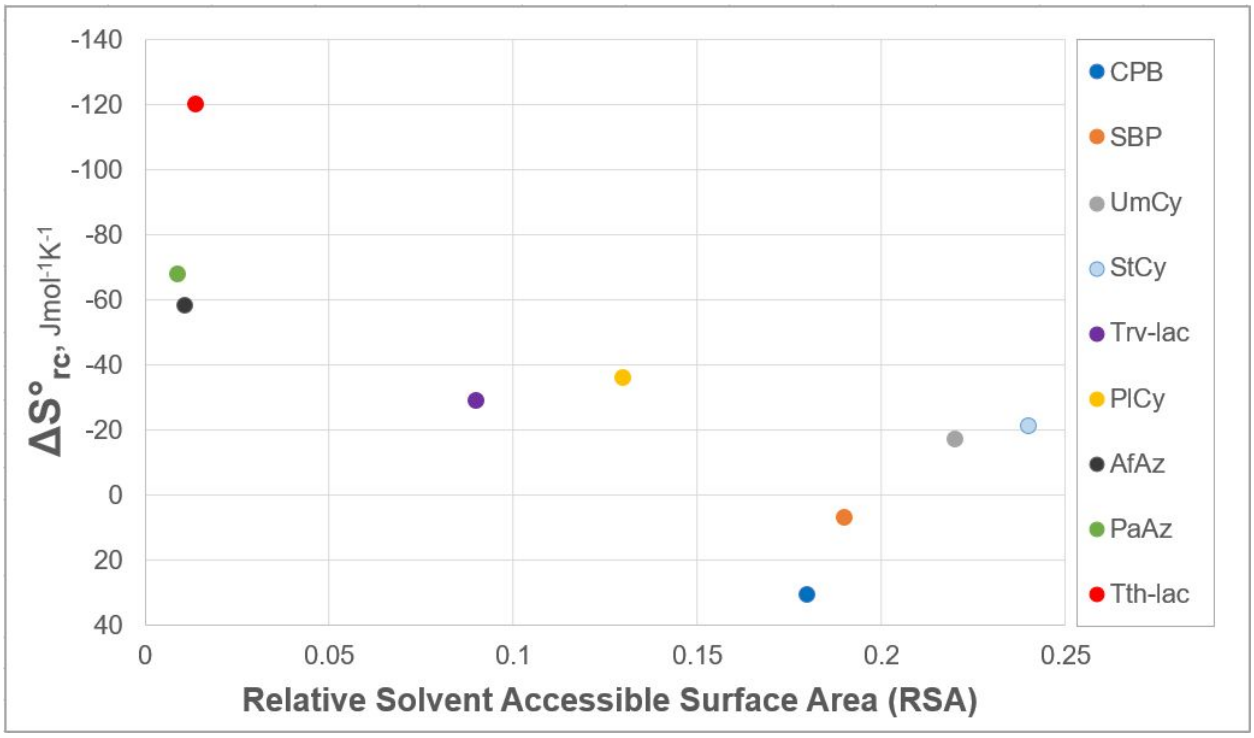

Figure S7. The correlation between reduction entropy ($\Delta S°_{rc}$, J $mol^{-1}K^{-1}$) and relative solvent accessible surface area (RSA)

Table S4. The solvent accessible surface area (Å²) and the relative solvent accessible surface area (RSA) of copper ligands in blue copper proteins (calculated with FreeSASA software [5]).
(The maximum SASA values for blue copper ligands are: His = 216.0 Å², Cys = 148 Å², Met = 203.0 Å² [6].)

CBP *(Cucumis sativus)*, [PDB: 2CBP]			**SBP *(Spinacea Oleracea)*, [PDB: 1F56]**			**Umecyanin *(Armoracia laphatifolia)*, [PDB: 1X9R]**		
Residue	**Solvent Accessible Surface Area (Å²)**	**RSA**	**Residue**	**Solvent Accessible Surface Area (Å²)**	**RSA**	**Residue**	**Solvent Accessible Surface Area (Å²)**	**RSA**
H39	13.31	0.06	H34	15.03	0.07	H44	22.65	0.10
H84	26.54	0.12	H79	26.73	0.12	H90	25.04	0.12
C79	0	0.00	C74	0	0	C85	0.1	0.001
M89	0	0.00	M84	0	0	Q95	0	0.00
Total	**39.85**	**0.18**	**Total**	**41.76**	**0.19**	**Total**	**47.79**	**0.22**
Stellacyanin *(Cucumis sativus)*, [PDB: 1JER]			**Laccase *(Trametes Versicolor)*, [PDB: 1GYC]**			**Plastocyanin *(Spinacea Oleracea)*, [PDB: 1AG6]**		
Residue	**Solvent Accessible Surface Area (Å²)**	**RSA**	**Residue**	**Solvent Accessible Surface Area (Å²)**	**RSA**	**Residue**	**Solvent Accessible Surface Area (Å²)**	**RSA**
H46	15.19	0.07	H395	5.32	0.02	H37	28.87	0.13
H94	37.11	0.17	H458	13.11	0.06	H87	0	0
C89	0.15	0.001	C453	0.12	0.001	C84	0	0
Q99	0	0	F463	0	0	M92	0.07	0.0003
Total	**52.45**	**0.24**	**Total**	**18.55**	**0.09**	**Total**	**28.94**	**0.13**
Azurin *(Alcaligenes faecalis)*, [PDB: 2IAA]			**Azurin *(Pseudomonas aeruginosa)*, [PDB: 5AZU]**			**Laccase *(Thermus thermophilus HB27)*, [PDB: 1JER]**		
Residue	**Solvent Accessible Surface Area (Å²)**	**RSA**	**Residue**	**Solvent Accessible Surface Area (Å²)**	**RSA**	**Residue**	**Solvent Accessible Surface Area (Å²)**	**RSA**
H46	0.06	0.0003	H46	0.65	0.003	H393	0.08	0.0004
H117	1.82	0.0084	H117	1.08	0.005	H450	0	0
C112	0	0	C112	0.02	0.0001	C445	2.05	0.014
M121	0.54	0.0027	M121	0.16	0.0008	M455	0	0
Total	**2.42**	**0.011**	**Total**	**1.91**	**0.009**	**Total**	**2.13**	**0.014**

■ References

1. Miyazaki, K (2005) A hyperthermophilic laccase from Thermus thermophilus HB27. Extremophiles 9(6):415-425. https://doi.org/10.1007/s00792-005-0458-z
2. Curtis JC, Sullivan BP, Meyer TJ. (1983) Hydrogen-Bonding-Induced Solvatochromism in the Charge-Transfer Transitions of Ruthenium(II) and Ruthenium(III) Ammine Complexes. Inorg Chem 22(2):224-236. https://doi.org/10.1021/ic00144a009
3. Nozaki Y and Tanford C (1971) The solubility of amino acids and to glycine peptides in aqueous ethanol and dioxane solutions. Establishment of a hydrophobicity scale. J Biol Chem 246(7):2211-7.
4. Zimmerman JM, Eliezer N, Simha R (1968) The characterization of amino acid sequences in proteins by statistical methods. J Theor Biol 21(2):170-201. https://doi.org/10.1016/0022-5193(68)90069-6
5. Simon Mitternacht (2016) FreeSASA: An open source C library for solvent accessible surface area calculation. F1000Research 5:189 https://doi.org/10.12688/f1000research.7931.1
6. Tien MZ, Meyer AG, Sydykova DK, Spielman SJ, Wilke CO (2013) Maximum Allowed Solvent Accessibilites of Residues in Proteins. PLoS ONE 8(11):e80635. https://doi.org/10.1371/journal.pone.0080635